






A Robust Cascaded Controller for Load Frequency Control in Renewable Energy Integrated Microgrid Containing PEV

Nessma M. Ahmed *, Mohamed Ebeed **, Khairy Sayed **
, Ayman Alhejji***, Ahmed Refai**

*Elect. Dep., Faculty of Technology and Education, Sohag University, Sohag, Egypt

**Department of Electrical Engineering, Faculty of Engineering, sohag University, sohag, Egypt

***Department of Electrical and Electronics Engineering Technology, Yanbu Industrial College, Yanbu Industrial City, Saudi Arabia

(nesma_mohamed_post@techedu.sohag.edu.eg, mebeed@eng.sohag.edu.eg, khairy_sayed@eng.sohag.edu.eg, alhejji@rcyci.edu.sa, ahmedrefai@eng.sohag.edu.eg)

‡Corresponding Author: Ayman Alhejji, Saudi Arabia, alhejji@rcyci.edu.sa

Received: 05.07.2022 Accepted: 20.11.2022

Abstract- The micro-grids (MGs) are widely incorporated in electrical systems for several economic, environmental, and technical benefits. The MGs suffer from high frequency oscillation in island mode due to scholastic nature of the load, renewable energy resources and plug-in electric vehicles (PEVs). This paper presents a cascade proportional derivative-proportional integral (PD-PI) controller tuned with a novel optimizer, named, gorilla troops optimization (GTO) algorithm for load frequency control of an isolated MG. The studied MG includes wind turbine generator (WTG), photovoltaic (PV) diesel engine generators (DEG), Fuel cell and PEV. Different scenarios are presented in this study to verify the robustness and sensitivity of the proposed PD-PI controller including different step load fluctuations, the wind speed and the solar irradiance variations. The results obtained by the PD-PI controller are compared with performance of the conventional a proportional–integral–derivative (PID) and PI controllers for mitigating the oscillation of the frequency in MG containing a PEV model. The simulation results depict the effectiveness of the proposed PD-PI controller in different scenarios.

Keywords Load Frequency Control; Cascade Controller; Renewable Energy Sources; Gorilla Troops Optimization.

1. Introduction

Energy plays a crucial role in the advancement of the economy and the raising of social expectations for basic comforts. Alternative energy sources, including solar, wind, fuel cells, and diesel engine generators, etc., have recently started to offer isolated communities and facilities more affordable, ecologically friendly, and higher-quality power sources. In order to create a micro-grid (MG), various small-scale generation resources are combined MG. An isolated MG runs independently of the primary power system [1]–[3]. Due to the MG's low inertia and the intermittent nature of the PV and WTG system's power supply, the system frequency may be critically impacted, which could lead to the collapse of the system. In such a case, load frequency control (LFC) is essential [4].

LFC task is to keep the system frequency variations within the defined limits by minimizing the mismatch between the power supply and the load demand. One of the most practical solutions to this issue is the use of the energy storage system s(ESSs), such as battery energy storage systems (BESS) and flywheel energy storage systems (FESS). The ESS is expensive and has a low energy density, which is why electrical vehicle (EV) technology is becoming more and more popular on a global scale [5]. The EV technology is frequently employed for frequency management in MGs that result from the mismatch between the supply and the load demand and the intermittent nature of renewable energy source (RES) due to its high energy density and bidirectional charging/discharging power regulation [6], [7].

MGs are a developed part of power systems that include renewable and conventional energy resources which have

been utilized to feed a certain small load in the system. Due to the variations in loads as well as the power generated by renewable energy resources resulting in high fluctuations in frequency. The load frequency control (LFC) in MGs is always a challenging task for the operators. Several controllers have been suggested for optimizing the LFC in the MGs. In [8]–[10] a fuzzy adaptive model predictive control (MPC) has been implemented for the LFC of the MG. For example, the influence of the MPC on the LFC has been studied under with adjusting the tuning parameter ‘Rw’. The authors in [11] proposed an adaptive fuzzy PID controller (AFPID) for the LFC model of the MG, and the parameters of this controller are optimized by the amended sine cosine method. An Integral Square Time Error evaluation criterion (ITSE) and Ziegler Nichols method have been applied for adjusting the parameters of the PID controller for the LFC of the MG [12], [13]. Y. Xu et al applied artificial sheep algorithm (ASA) for LFC of an MG which includes a hydropower energy storage with renewable resources [14]. Electronic load controller (ELC) consisting of hydro energy sources, induction generator and synchronous generator is used to regulate the frequency of the MG as provided in [15]. The authors in [16] proposed type-II fuzzy PID to regulate the LFC in a two area AC microgrid where the parameters of this controller were optimized by the improved-slap swarm optimization. The particle swarm optimization along with artificial neural network was proposed to adjust the PID control parameters for LFC in MG [17]. The lightning attachment procedure optimization (LAPO) is served for optimizing the PID controller of the LFC in a hybrids MG [18]. The authors in proposed a linear, quadratic Gaussian with the PID controller and (LQG) controller for regulating the frequency in two-area system [19]. A two-level control mechanism has been proposed for reducing the fluctuations in a wind-diesel MG which include fuzzy logic approach (FLA) to update the parameters of Proportional Integral (PI) controller [20]. In [21], two different controllers are used which are the cascade PD-PI controller and the conventional PID controller of the AGC system for a multi-unit, two-zone interconnected thermal power system. A 1% progressive load disturbance is applied, and a new global search optimization technology called TLBO is used for effective tuning of the controllers. The PD-PI cascade controller is shown to distinguish it from the PID controller. For a mutant based two-area interconnected system, a novel GOA based cascaded fuzzy PD-PI controller is presented in [22] to improve frequency stability. The power of the FPD-PI controller over other controllers has been demonstrated, demonstrating that the GOA and FPD-PI cascading controller technology is superior than other controllers.

GTO is a novel meta-heuristic optimization algorithm described in [23]–[25]. The GTO has been used to solve numerous optimization challenges involving solar photovoltaic unit parameters [26]. The design of the cascaded PI-fractional order PID controller for the LFC was determined by the GTO for the LFC [27]. The solution offered by the authors in applied the GTO for optimizing the management of the reservoir operation. Moreover, As illustrated in [28], the GTO was used to determine the variables of proton membrane fuel cells.

The proposed microgrid system, together with a PEV charging station, has been taken into consideration in the current article about a study on load frequency regulation. Multiple sources, including wind, fuel cells, solar cells, and energy storage sources, have also been taken into consideration. The cascade proportional derivative-proportional integral (PD-PI) controllers are evaluated for their optimal gains using an optimization technique inspired by the collective intelligence of natural organisms in nature, called the gorilla troops optimization (GTO) algorithm. By contrasting the outcomes with conventional PI and PID controllers, the system's dynamic performance is investigated. The remainder of the framework is structured as follows: Section 2 is devoted to the modelling of the component of the MGs. Section 3 describes the layouts of the analysed system. Section 4 discusses the proposed PD-PI cascade controller. Section 5 presents an overview about the GTO algorithm. Section 6 demonstrates the simulation results. Finally, section 7 concludes with a summary.

2. Studied System Model

2.1. Electric Vehicle Modelling

With the widespread use of electric vehicles to replace traditional fossil fuel-powered vehicles, additional functions have been introduced to govern the EVs increase power system response, efficiency, and reliability. One of the most important roles is to maintain power MG frequency stable during a step change in generated and absorbed power from renewable energy sources (RES) and associated loads. Fig. 1 depicts a sophisticated dynamic model of EVs that was supplied in this work for frequency response study, as indicated in[29], [30]. Furthermore, the Nernst equation is frequently introduced to represent the relationship between the state of charge (SOC) and the open-circuit voltage (OCV) and of linked EVs as depicted in Table 1 [29], [31]–[36].

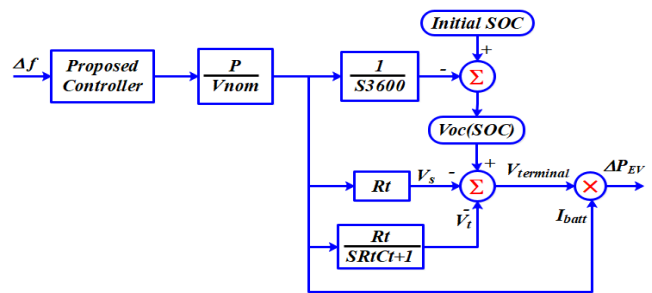


Fig. 1. Modelling of the PEV.

2.2. Wind Turbine Generation

To simulate nature of the output power of the of the wind units, this study employs a simple wind power plant model based on the first-order transfer function as listed in Table 1 [16], [17], [37].

2.3. Photovoltaic

A photovoltaic unit includes a PV panel, a DC-DC converter, a maximum power point tracker (MPPT), and a

filter circuit [16], [38]. The mathematical form of photovoltaics is shown in Table 1.

2.4. Diesel Generator (DG)

A diesel engine generator is typically installed in remote locations or utilized as an alternate contingency power source to deliver power while the power outage in the main grid takes place. Furthermore, DEGs are employed not only as backup or emergency units, but also as supplemental power sources to compensate for the intermittent nature of RESs in the stand-alone microgrids. Aside from that, the DEG offers quick start-up, great efficiency, and low maintenance costs. Furthermore, with its power control mechanism, it has the potential to rapidly adjust its generation in response to load differences [30], [38]. The governor is the initial block in the DEG's transfer function, accompanied by the DG block, and finally the saturation block (see Fig. 2). The governor manages the condition of the valve (ΔXG) based the frequency variation (Δf), R indicates the droop, and ΔP_{DEG} represents the increase in the DEG output power.

TABLE 1: Transfer functions for the system model

Subsystem	Transfer Function
PEV	$V_{oc}(SOC) = V_{nom} + S \frac{RT}{F} \ln \left(\frac{SOC}{C_{nom} - SOC} \right)$
WTG	$TF_{WT}(s) = \frac{k}{\tau_w s + 1}$
PV	$TF_{PVi}(s) = \frac{k}{\tau_{PVi} s + 1}$ $TF_{PVc}(s) = \frac{k}{\tau_{PVc} s + 1}$
DEG	$TF_{DEGt}(s) = \frac{k}{\tau_{Dt} s + 1}$ $TF_{DEGg}(s) = \frac{k}{\tau_{Dg} s + 1}$
BESS	$TF_{BESS}(s) = \frac{k}{\tau_{BESS} s + 1}$
FC	$TF_{FCt}(s) = \frac{k}{\tau_{FCt} s + 1}$ $TF_{FCi}(s) = \frac{k}{\tau_{FCi} s + 1}$ $TF_{FCc}(s) = \frac{k}{\tau_{FCc} s + 1}$

The ramp rate limit of the DEG controls the rate at which the output power of the DEG can be altered in order to meet the power balance. The generator and governor time constants are τ_{Dt} and τ_{Dg} , respectively [16]. The diesel generator can be represented mathematically as shown in Table 1.

2.5. Battery Energy Storage System (BESS)

BESS is a type of energy storage, which is coupled in the control loop and activated by the controller signal. They serve as a source or a burden to the system, depending on the requirements. The storage sections of the power system are meant to work in the nonlinear zone [16], [38], which can be described mathematically as indicated in Table 1.

2.6. Fuel Cell (FC)

An FC is an important component and widely integrated into the MG that has lower emissions and higher efficiency. The first-order function generator of the FC is listed in Table 1 [38].

3. The Layout of the System

The power balance between generation supply and demand determines frequency stability. The microgrid frequency deviates from the nominal value when an imbalance occurs. As a result of that, the microgrid control centre is in charge of restoring the power balance between generation and demand [15], [38]. For instance, to investigate the frequency stability issue, a dynamic analysis of the islanded microgrid is illustrated in Fig. 2. In addition, the cascade PD-PI control is designed for EVs. The frequency regulation problem is not affected by the wind or solar PV power. Thus, the perturbations of the investigated MG are the wind, PV, and load powers. On the other hand, the DEG, FC, and BESS sources help to control the microgrid frequency. As a result, in microgrid, a proper control strategy is required. The cascade PD-PI controller is a novel controller developed in this framework that combines the PD and PI controllers.

The following is the relationship between microgrid frequency deviation and inertia constant:

$$\Delta f = 1Ms + D[\Delta P_{mg} - \Delta P_{Load}] \quad (1)$$

Where:

$$\Delta P_{mg} = \Delta P_{PV} + \Delta P_{Wind} + \Delta P_{DGE} + \Delta P_{FC} + \Delta P_{BESS} + \Delta P_{EV} \quad (2)$$

The microgrids generation and load power changes are represented by ΔP_{mg} and ΔP_{Load} , respectively. The inertia and damping constants of the MG are denoted by M and D , respectively. The time constants of the wind, FC, and BESS are displayed in Fig. 2 as τ_w , τ_{FC} , and τ_{BESS} respectively. Where k is the gain of the system in the Fig 2. DEG governor and turbine time constants are τ_{Dg} and τ_{Dt} , respectively. The DG governor speed regulation coefficient is R . In addition, τ_{PVi} , τ_{PVc} , τ_{FCi} , and τ_{FCc} denote the inverter and interconnector time constants, for PV and FC respectively. Appendix A contains the values of the investigated microgrid parameters.

4. The Proposed PD-PI Cascade Controller Design

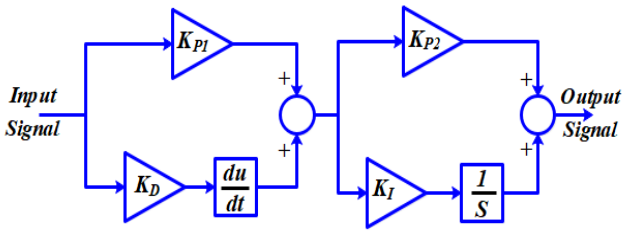


Fig. 2 Structure for PD-PI cascade controller

Figure. 3 depicts the configuration of a PD-PI cascade controller incorporated in both sections of the system model [22]. The performance of this controller is determined by parameters such as K_{P1} , K_D , K_{P2} , K_I and the tuning controller's gain values are determined using the GTO optimization technique. The controller is programmed with this technique to obtain the best controller gains and a greater dynamic response from the PD-PI cascade controlled for automatic generation control (AGC) [33].

The transfer function is provided by Eq (3). In terms of the s-domain performance of the PD-PI cascade controller.

$$TF_{PD-PI} = \{(K_{P1} + SK_D) * (K_{P2} + K_I S)\} \quad (3)$$

The PD-PI cascade controller was selected for AGC in this study due to its improved system performance. The ACEs are the control input signals, and the reference power settings of individual generating units are the control output signals. The LFC, a subset of AGC, has been implemented in electric power systems for several years to sustain constant frequency and tie-line capacity with zero steady-state error. The traditional PI and PID controllers are nominated for their easy implementation and better performance results. Traditional

controllers such as PI and PID can effectively eliminate steady-state error, but they fail when the gadget intricacy grows due to many interconnects and non-linearity.

4.1 Objective Function

Without properly adjusting the controller's parameters, we cannot expect appropriate performance. The proper setting of a controller's parameters in accordance with the system is crucial to its effective operation. The definition of an acceptable objective function is crucial for directing optimization algorithms in the direction of the designer's objectives. The fundamental challenge in addressing the LFC problem is ensuring system stability and accuracy and quickly correcting steady-state faults.

To determine the best value for the control parameters, the integral of time multiplied absolute error (ITAE) is employed as the objective function. The following diagram shows the objective function J for the linked power system's controller parameter optimization.

$$F = \int_0^t (\Delta f)^2 \cdot dt \quad (4)$$

The frequency variation in MG is denoted by Δf , and the simulation time is denoted by t.

5. Artificial Gorilla Troops Optimizer

Metaheuristics are effective methods for tackling optimization problems, and most of them are based on the collective intelligence of natural organisms. The artificial gorilla troop optimizer is an optimization method simulates the social interaction and life style of gorilla tribes in nature. [23], [26].

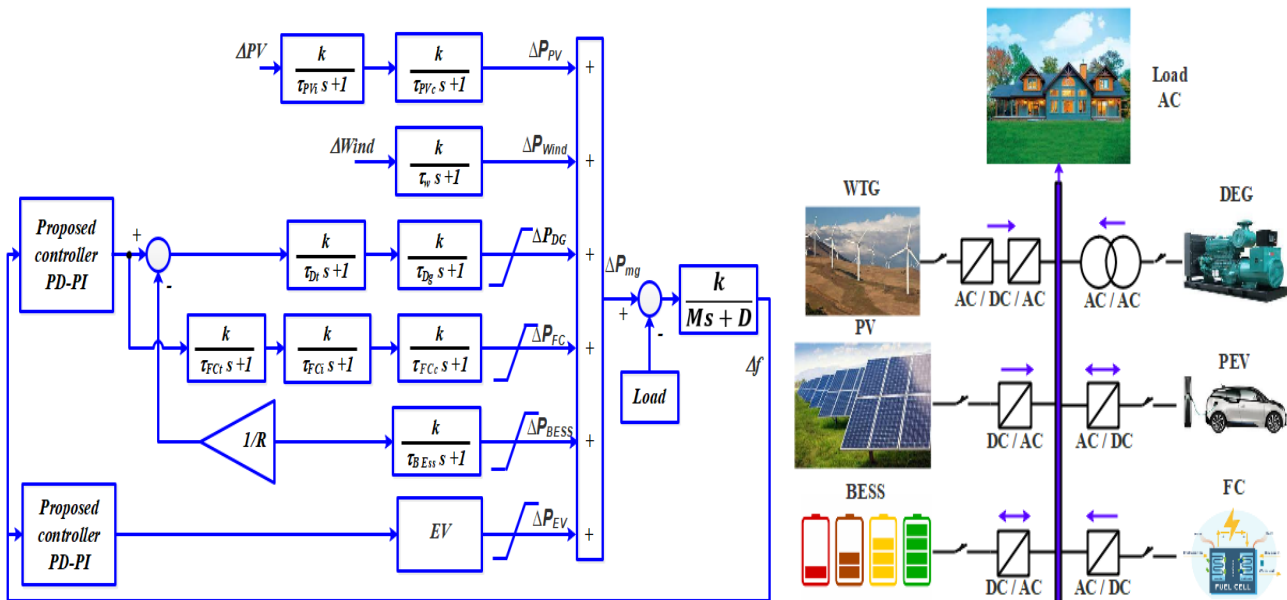


Fig. 3 Diagram of the MG under studied and the physical layout of the system.

The social existence of gorillas is mathematically described in this programmer, and novel methods for exploration and exploitation are devised. Fifty-two typical benchmark functions and seven engineering issues to evaluate the GTO. The proposed methodology was statistically compared against numerous current metaheuristics using Wilcoxon rank-sum method and Friedmans test. The results clearly demonstrate that the GTO outperforms competing algorithms on the majority of benchmark functions, especially in high-dimensional issues. The findings have shown that the GTO outperforms other metaheuristics in terms of performance [23], [26], [39].

5.1 Exploration Phase

In this algorithm the candidate solutions are gorillas for all optimization operation stages, while the best candidate solution is considered as a Silverback gorilla. The exploratory research phase includes migrating to an undisclosed place to increase GTO investigation, motion to other gorillas to rise the balance between exploration, and exploitation. In addition to that the migration of gorillas in the direction of a known location to enhance the capability of the GTO. When (Rand < a) parameter (p), the migration to an unknown location approach is chosen. In addition, if (Rand ≥ 0.5), a migration to a designated site is selected, whereas if (Rand ≤ 0.5), a migration to other gorillas is selected. The following are three mathematical expressible exploration strategies:

$$GX(t + 1) = \begin{cases} (UL - LL).r1 + LL, & rand < p, \\ (r2 - C).X_r(t) + L.H, & rand \geq 0.5, \\ X(i) - L.(L.(X(t) - GX_r(t)) + r3.(X(t) - GX_r(t))) & < 0.5 \end{cases} \tag{5}$$

where X (t) and GX (t+1) are the location of current gorilla and the candidate's gorilla position at the next t iteration, respectively, and Rand, r1, r2, and r3 are random values in the range of 0 to 1, and Rand, r1, r2, and r3 are random values in the range of 0 to 1. Before the optimization technique indicates the likelihood of picking the migration strategy to an unidentified site, the parameter (p) must be in the range of 0 to 1. One gorilla from the total population and one of the vectors of randomly assigned gorilla candidate locations are represented by the variables Xr and GXr, accordingly. The lower and upper boundaries of the variables are marked by LL and UL, accordingly. The variables (C, L, and H) are mathematically described using (7), (9) and (10) correspondingly [39].

$$C = F \times (1 - It/MaxIt), \tag{6}$$

$$F = \cos(2 \times r4) + 1, \tag{7}$$

$$L = C \times l, \tag{8}$$

$$H = Z \times X(t), \tag{9}$$

$$Z = [-C, C] \tag{10}$$

Where both It and MaxIt denote the optimization method's current and total repetition values, whereas cos and r4 signify the function generator and randomized value systems within [0-1]. The l and Z denote for random variables in the [-1, 1] and [-C, C] ranges. The cost of all GX answers is determined at the end of the exploration phase, and if the cost of GX (t) is less than the cost of X (t), the GX (t) answer replaces the X (t) answer as Silverback (the best option).

5.2 Exploitation Phase

Chasing the Silverback and battling for mature females is two tactics addressed during GTO's optimising procedure. One of the two techniques, as illustrated in the next section, can be chosen by matching the (C) value in Eq. (7) With variable (W) (which can be changed). The Silverback gorilla oversees a group of gorillas, making decisions and directing them to food sources. If Cgeq W is present, this is the strategy to take. A diagrammatic description of this behaviour is referred to as an Eq (11).

$$GX(t + 1) = L.M.(X(t) - X_{silverback}) + X(t) \tag{11}$$

The gorilla locations are supplied by X (t), while the Silverback gorilla support implementation is provided by Silverback.

$$M = \left(\left| \left(\frac{1}{N} \sum_{i=1}^N GX_i(t) \right)^g \right|^{(1/g)} \right) \tag{12}$$

GXi (t) represents the location of each prospective gorilla's variable in iteration (t), where (N) is the number of gorillas.

$$g = 2^L \tag{13}$$

L can be given by Eq. (9). Competing for adult females is the second method for the exploitation phase if (C < W) is applied. Young gorillas compete furiously with other males for adult females when they reach adulthood. Eq. (14) Can be used to quantitatively represent these characteristics.

$$GX(i) = X_{silverback} - (X_{silverback} \times Q - X(t) \times Q) \tag{14}$$

$$\times A \tag{15}$$

$$Q = 2 \times r5 - 1, \tag{15}$$

$$A = \beta \times E, \tag{16}$$

$$E = \begin{cases} N_1 rand \geq 0.5 \\ N_2 rand < 0.5 \end{cases} \tag{17}$$

The symbol (Q) stands for the applied pressure specified by Eq. (15), while the notation r5 stands for random ranging between 0 and 1. The parameter A, which is a vector indicating the level of violence in a combat, can be calculated using Eq. (16). To simulate the act of violence on the answer dimensions, Eq. (16) Use (E). Before the optimization procedure starts, the parameter is set to a certain value.

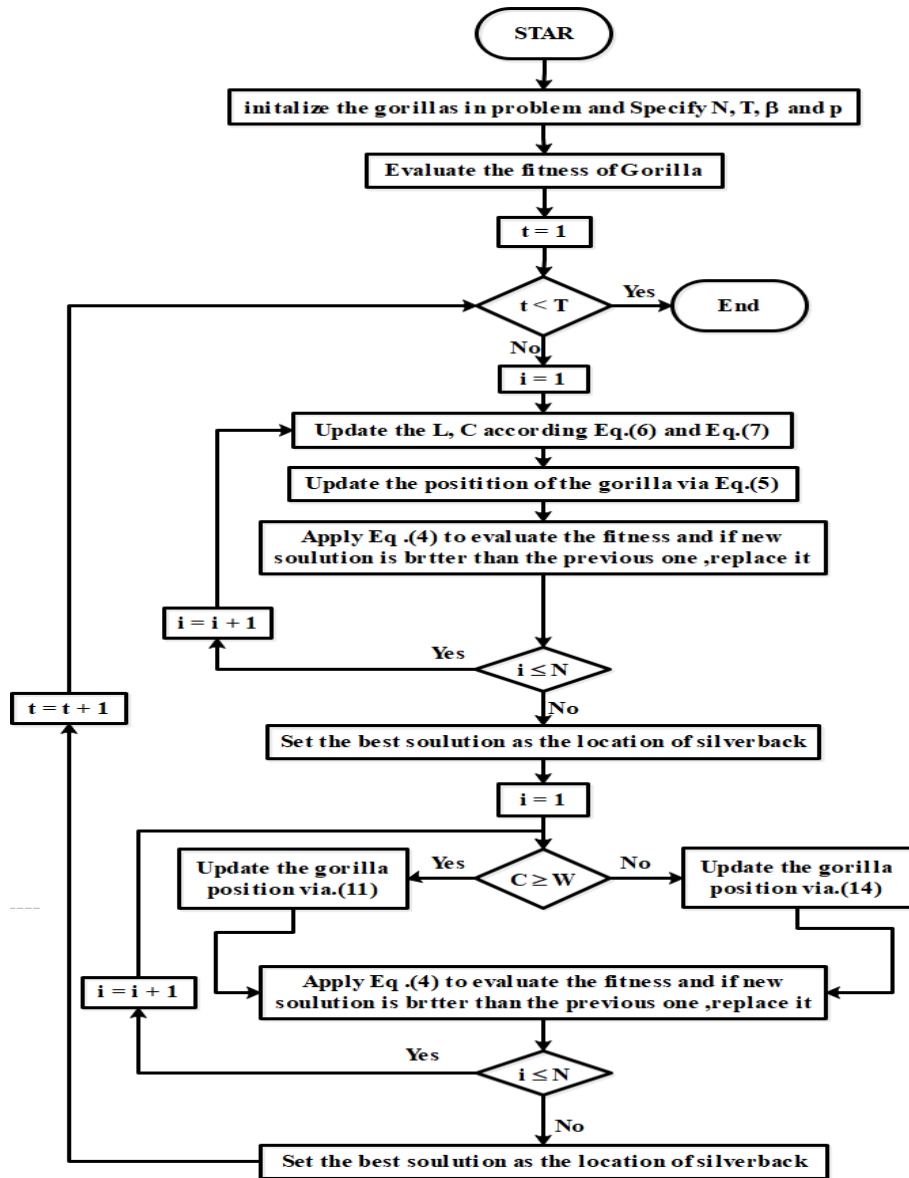


Fig. 4 The proposed GTO technique flowchart. [26]

The optimization problem of all GX answers is assessed at the end of the define stage, and if the value of GX (t) is less than the cost of X (t), the GX (t) answer will replace the X (t) answer as the best choice (Silverback). Fig. 4 depicts the basic stages of the suggested GTO for simulation and optimization of proposed Scheme models.

6. Model Simulation Results

The MG frequency response is simulated in time domain and presented in this section. When compared to other controllers, the suggested GTO algorithm-based PI-PD cascade controller performs better. Two different MG working situations have been taken into consideration to show the usefulness of the suggested controller. In Appendix A, the parameters of the proposed system are listed. The following specs were used for the personal system where all simulations were run in the MATLAB/SIMULINK 2018 environment: 2.50GHz Intel Core i7 CPU with 8GB RAM. GTO parameters: population size = 30; maximum number of iterations = 50. The frequency results of the PD-PI cascade

controller system are evaluated and compared to PID and PI controllers. Two cases that were studied are as follows:

6.1 Case1: Step Change of the Load

In this case a 20% p.u perturbation of load was applied as shown in Figure 5. In the case a perturbation of the load was imposed when the simulation time started at (t = 0 s) to test the efficacy of the proposed PD-PI serial controller. This carried out without any changes in the speed of the wind turbines or the solar radiation available to generate photovoltaic energy, which means the system can be considered in a stable state. The proposed model has been tested in simulations involving an energy storage system, as illustrated in Figure 5 (b) C-BESS control signals that regulate the operation and supply energy from the battery stock and from the batteries to the micro-grid and back as needed. The stability of PBESS power output is shown in Fig. 5(c). Figure 5(d) shows the fluctuations of the stand-alone MG frequency with PI, PID and PD-PI sequence controllers. It is obvious that

the proposed controller is superior for reducing the oscillation of the frequency compared with other controllers. The optimal parameters of the proposed PD-PI, PI and PID controllers are listed in Table 2.

Table 2 Optimized System Parameters Values of Case (1)

Parameters / Controller		PI	PID	PD-PI
(1)	KP ₁	2.07471	7.90253	10
	KD ₁	-	1.35550	2.28397
	KP ₂	-	-	2.30183
	KI ₁	3.97734	10	10
(2)	KP ₁	0.19338	0	0.474664
	KD ₁	-	9.55639	2.54814
	KP ₂	-	-	2.05229
	KI ₁	4.47895	10	2.42323
Objective Function		4.67060	1.33777	0.138792

6.2 Case2: A Sequence Step Change of the load, the wind and the solar PV power

In this case, the performance of system was tested with the proposed controller at the variation of the load demand, and the produced power by wind turbine and the PV unit (ΔP_{Wind} , ΔP_{Pv}) as depicted in Figure 6. According to Figure 6, the load demand is varied between [0.1-0.3] while the step change of the output power of the wind and the PV units are in range of [0.1-0.25]. Figure 7 illustrates the response to the change in frequency of the micro-grid using the PI, PID and

PD-PI sequential controllers. According to Figure 7, it clear that the oscillation in frequency and the settling time is decreased considerably with inclusion of the proposed controller compared with the other controllers. Table 3 lists the optimal parameter values for the PI, PID and PD-PI cascaded controllers.

Table 3 Optimized System Parameters Values of Case (2)

Parameters / Controller		PI	PID	PD-PI
(1)	KP ₁	1.85391	6.36389	1.99138
	KD ₁	--	1.23281	2.43939
	KP ₂	--	--	1.05564
	KI ₁	1.49305	10	4.86525
(2)	KP ₁	5.80870	2.42776	1.84776
	KD ₁	--	0.658473	2.78619
	KP ₂	--	--	0.660081
	KI ₁	10	10	8.05321
Objective Function		19.96704	2.97874	2.48294

Figure 8 (a,b,c,d,e) represents the detailed of the frequency deviation signal generated by the proposed system, depicting the superiority of the proposed PD-PI sequential control system. Despite the fact that the diversity of renewable energy resources, including wind and solar, has led to changes, time stabilization, overrun and frequency reduction have all been discussed.

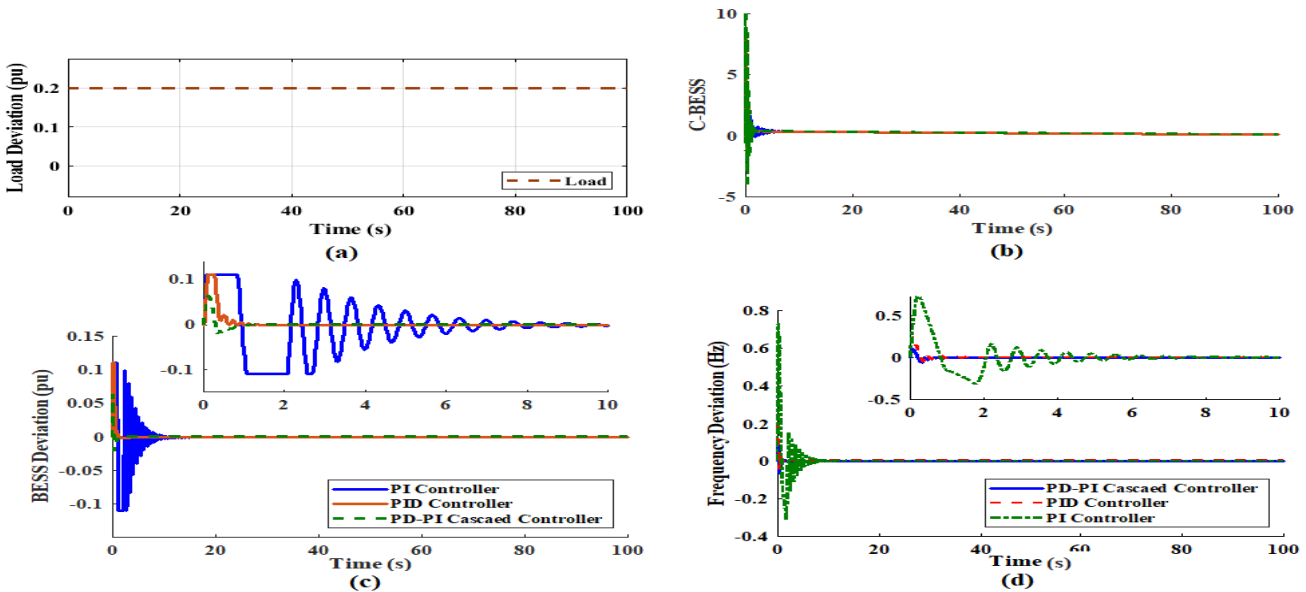


Fig. 5 The shows the results for BESS for load fluctuations using PI, PID, and PD-PI cascade controllers: (a) step-change load fluctuation in p.u, (b) C-BESS control input, (c) BESS energy, and (d) frequency response.

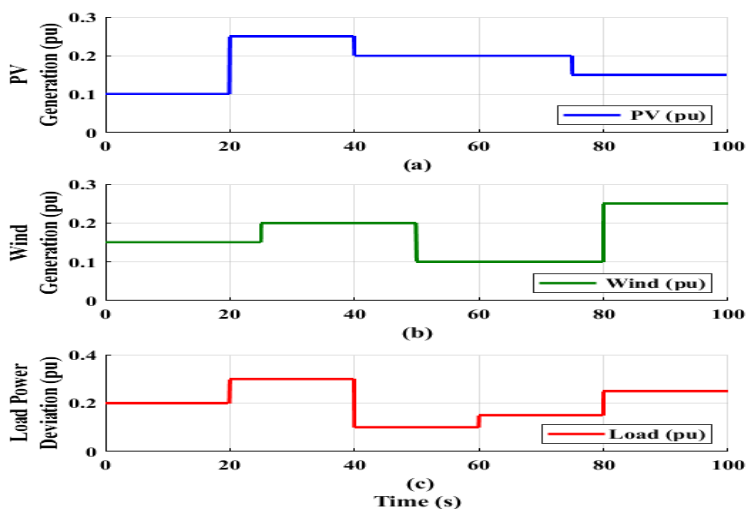


Fig. 6 Microgrid disturbances and frequency response for case (2) (a) PV output power. (b) Wind output power. (c) Pattern of considered load disturbance.

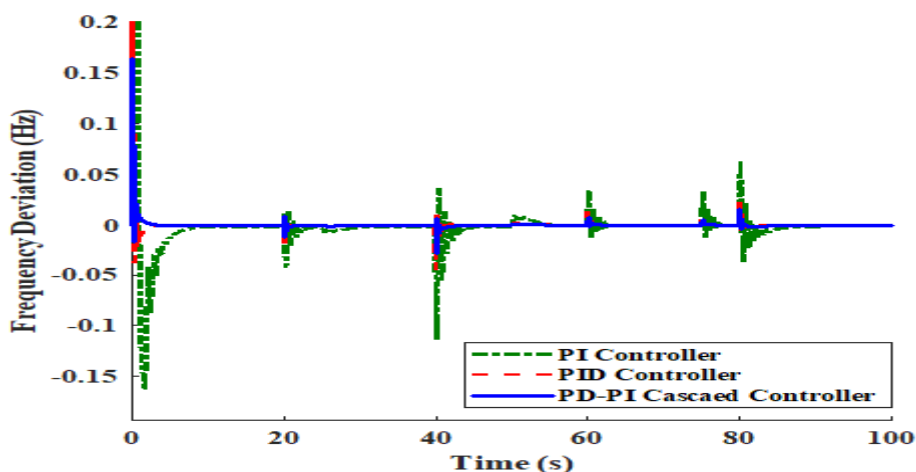


Fig. 7. Resulted frequency responses of the case 2

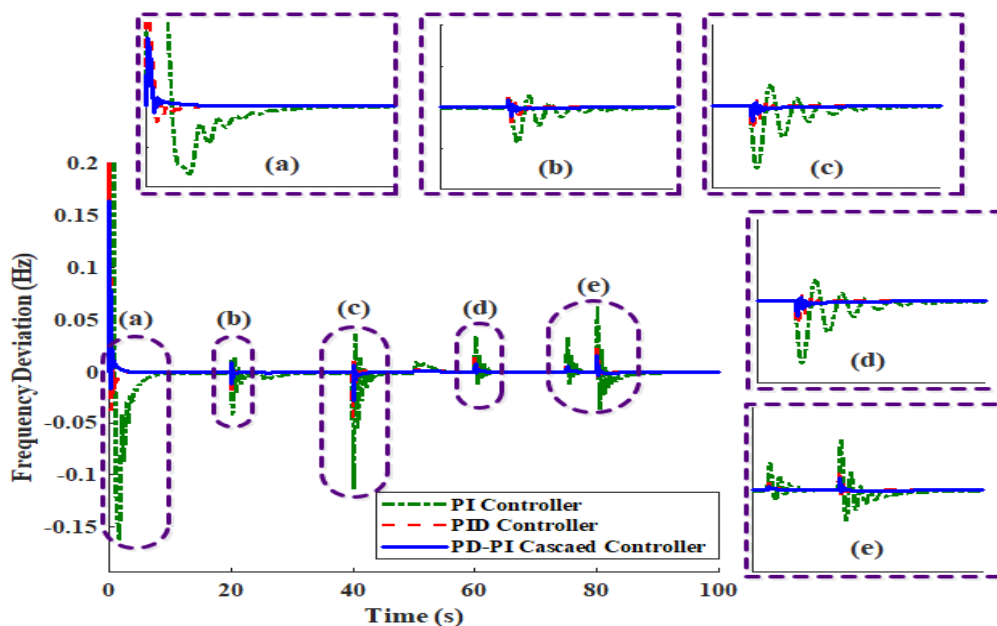


Fig. 8. Zoom of frequency deviations of the MG for case 2.

7. Conclusions

For the LFC of incorporating EVs, a PI-PD cascade controller has been suggested in this article. A recently developed GTO method has been used to maximize the controller gains. Various MG operating situations have been taken into consideration to validate the viability of the suggested controller. In each of the cases, the controller's performance was compared to that of other well-known controllers. The proposed controller performs remarkably well in terms of the lowered performance index values corresponding to each situation, according to simulation findings. The system's performance was evaluated with the implementation of the PD-PI cascade controller and the results were compared to those achieved by the PID and PI controllers. The performance is evaluated under different scenarios of variations of the load, the PV and WT powers. The simulation results show that the proposed controller is superior compared with the conventional of the PID and PI controllers in terms of reducing the oscillation of the system frequency.

Appendix A

Design Parameters	
$V_{nom} (V) = 364.8$	$\tau_{PV_i} = 0.04$
$C_{nom}(Ah) = 66.2$	$\tau_{PVC} = 0.004$
$R_s(ohms) = 0.074$	$\tau_w = 1.5$
$R_t(ohms) = 0.047$	$\tau_{Dt} = 0.4$
$C_t(farad) = 703.6$	$\tau_{Dg} = 0.08$
$RT / F = 0.02612$	$\tau_{BESS} = 0.1$
$SOC = 95\%$	$\tau_{FCt} = 0.26$
$C_{batt}(kWh) = 24.15$	$\tau_{FCi} = .004$
$K=1$	$\tau_{FCc} = 0.004$

Appendix B

NOMENCLATURE	
PEVs	Plug-in electric vehicles
GTO	Gorilla troops optimization
PD-PI	Proportional derivative-proportional integral
DG	Distributed generator
PV	Photovoltaic
MG	micro-grid
BESS	Battery Energy Storage System
ESS	Energy Storage System
LFC	Load frequency control
RES	Renewable energy sources
OCV	The open-circuit voltage
SOC	State of charge
AGC	Automatic generation control
PID	Proportional-Integral-Derivative
ITAE	Integral of time multiplied absolute error

References

- [1] D. K. Lal and A. K. Barisal, "Load Frequency Control of AC Microgrid Interconnected Thermal Power System," *IOP Conf. Ser. Matter. Sci. Eng.*, vol. 225, p. 012090, 2017, doi: 10.1088/1757-899x/225/1/012090.
- [2] M. W. Siti, D. H. Tungadio, Y. Sun, N. T. Mbungu, and R. Took, "Optimal frequency deviation control in microgrid interconnected systems," *IET Renew. Power Gener.*, vol. 13, no. 13, pp. 2376–2382, 2019, doi: 10.1049/iet-rpg.2018.5801.
- [3] A. Ghosh, A. K. Ray, M. Nurujjaman, and M. Jamshidi, "Voltage and frequency control in conventional and PV integrated power systems of a particle swarm optimized Ziegler–Nichols based PID controller," *SN Appl. Sci.*, vol. 3, no. 3, 2021, doi: 10.1007/s42452-021-04327-8.
- [4] T. Mohamed, H. Abubakr, M. Hussein, and G. Shabib, "Load Frequency Controller Based on Particle Swarm Optimization for Isolated Microgrid System," *Int. J. Apple. Energy Syst.*, vol. 1, no. 2, pp. 69–75, 2019, doi: 10.21608/ijaes.2019.169953.
- [5] S. Padhy, P. R. Sahu, S. Panda, S. Padmanaban, J. M. Guerrero, and B. Khan, "Marine predator algorithm based PD-(1+PI) controller for frequency regulation in multi-microgrid system," *IET Renew. Power Gener.*, vol. 16, no. 10, pp. 2136–2151, 2022, doi: 10.1049/rpg2.12504.
- [6] M. H. Khooban, T. Niknam, M. Shasadeghi, T. Dragicevic, and F. Blaabjerg, "Load Frequency Control in Microgrids Based on a Stochastic Noninteger Controller," *IEEE Trans. Sustain. Energy*, vol. 9, no. 2, pp. 853–861, 2018, doi: 10.1109/TSTE.2017.2763607.
- [7] A. Hassan, M. Aly, A. Elmelegi, L. Nasrat, M. Watanabe, and E. A. Mohamed, "Optimal Frequency Control of Multi-Area Hybrid Power System Using New Cascaded TID-PIAD μ N Controller Incorporating Electric Vehicles," *Fractal Fract.*, vol. 6, no. 10, p. 548, 2022, doi: 10.3390/fractalfract6100548.
- [8] S. Kayalvizhi and D. M. Vinod Kumar, "Load frequency control of an isolated micro grid using fuzzy adaptive model predictive control," *IEEE Access*, vol. 5, no. C, pp. 16241–16251, 2017, doi: 10.1109/ACCESS.2017.2735545.
- [9] B. Mohammadi-ivatloo, "Provision of Frequency Stability of an Islanded Microgrid Cascade Controller," 2021.
- [10] K. S. Rajesh and S. S. Dash, "Load frequency control of the autonomous power system using adaptive fuzzy based PID controller optimized for improved sine cosine algorithm," *J. Ambient Intell. Humaniz. Comput.*, vol. 10, no. 6, pp. 2361–2373, 2019, doi: 10.1007/s12652-018-0834-z.

- [11] A. A. Abou El-Ela, R. A. El-Sehiemy, A. M. Shaheen, and A. E. G. Dab, "Enhanced coyote optimizer-based cascaded load frequency controllers in multi-area power systems with renewable," *Neural Comput. Appl.*, vol. 8, 2021, doi: 10.1007/s00521-020-05599-8.
- [12] G. Malleshm, S. Mishra, and A. N. Jha, "Ziegler-Nichols based controller parameter tuning for load frequency control in a microgrid," *Proc. - 2011 Int. Conf. Energy, Autom. Signal, ICEAS - 2011*, pp. 335–342, 2011, doi: 10.1109/ICEAS.2011.6147128.
- [13] D. C. Das, A. K. Roy, and N. Sinha, "GA based frequency controller for solar thermal-diesel-wind hybrid energy generation/energy storage system," *Int. J. Electr. Power Energy Syst.*, vol. 43, no. 1, pp. 262–279, 2012, doi: 10.1016/j.ijepes.2012.05.025.
- [14] P. Sanki and M. Basu, "New approach in two-area interconnected AGC, including various renewable energy sources using PSO," *Turkish J. Electr. Eng. Comput. Sci.*, vol. 26, no. 3, pp. 1491–1504, 2018, doi: 10.3906/elk-1707-241.
- [15] R. K. Khadanga, S. Padhy, S. Panda, and A. Kumar, "Design and Analysis of Tilt Integral Derivative Controller for Frequency Control in an Islanded Microgrid: A Novel Hybrid Dragonfly and Pattern Search Algorithm Approach," *Arab. J. SCI. Eng.*, vol. 43, no. 6, pp. 3103–3114, 2018, doi: 10.1007/s13369-018-3151-0.
- [16] A. H. Yakout, H. Kotb, H. M. Hasanien, and K. M. Aboras, "Optimal Fuzzy PIDF Load Frequency Controller for Hybrid Microgrid System Using Marine Predator Algorithm," *IEEE Access*, vol. 9, pp. 54220–54232, 2021, doi: 10.1109/ACCESS.2021.3070076.
- [17] R. K. Khadanga, A. Kumar, and S. Panda, "A novel sine augmented scaled sine cosine algorithm for frequency control issues of a hybrid distributed two-area power system," *Neural Comput. Appl.*, vol. 33, no. 19, pp. 12791–12804, 2021, doi: 10.1007/s00521-021-05923-w.
- [18] N. Jalali, H. Razmi, and H. Doagou-Mojarrad, "Optimized fuzzy self-tuning PID controller design based on Tribe-DE optimization algorithm and rule weight adjustment method for load frequency control of interconnected multi-area power systems," *Appl. Soft Comput. J.*, vol. 93, p. 106424, 2020, doi: 10.1016/j.asoc.2020.106424.
- [19] N. K. Kumar and V. Indragandhi, "Analysis on various optimization techniques used for load frequency control in power system," *Serbian J. Electr. Eng.*, vol. 15, no. 3, pp. 249–273, 2018, doi: 10.2298/sjee1803249k.
- [20] P. Sanki, S. Mazumder, M. Basu, P. S. Pal, and D. Das, "Moth Flame Optimization Based Fuzzy-PID Controller for Power-Frequency Balance of an Islanded Microgrid," *J. Inst. Eng. Ser. B*, vol. 102, no. 5, pp. 997–1006, 2021, doi: 10.1007/s40031-021-00607-4.
- [21] S. Panda, N. P. Patidar, and M. Kolhe, "Cascaded PD-PI controller for active power frequency control of two-Area multi-unit power system," *2016 IEEE Int. Conf. Power Renew. Energy, ICPRE 2016*, pp. 251–254, 2017, doi: 10.1109/ICPRE.2016.7871210.
- [22] D. Tripathy, N. D. Choudhury, and B. K. Sahu, "A novel cascaded fuzzy PD-PI controller for load frequency study of solar-thermal/wind generator-based interconnected power system utilizing a grasshopper optimisation algorithm," *Int. J. Electr. Eng. Educ.*, pp. 1–18, 2020, doi: 10.1177/0020720920930365.
- [23] B. Abdollahzadeh, F. Soleimanian Gharehchopogh, and S. Mirjalili, "Artificial gorilla troops optimizer: A new nature-inspired metaheuristic algorithm for global optimization problems," *Int. J. Intell. Syst.*, vol. 36, no. 10, pp. 5887–5958, 2021, doi: 10.1002/int.22535.
- [24] E. H. Houssein, M. R. Saad, A. A. Ali, and H. Shaban, "An efficient multi-objective gorilla troops optimizer for minimizing energy consumption of large-scale wireless sensor networks," *Expert Syst. Appl.*, vol. 212, no. February 2022, p. 118827, 2023, doi: 10.1016/j.aswan.2022.118827.
- [25] T. Wu *et al.*, "A Modified Gorilla Troops Optimizer for Global Optimization Problem," *Appl. Sci.*, vol. 12, no. 19, 2022, doi: 10.3390/app121910144.
- [26] A. Ginidi, S. M. Ghoneim, A. Elsayed, R. El-Sehiemy, A. Shaheen, and A. El-Fergany, "Gorilla troops optimizer for electrically based single and double-diode models of solar photovoltaic systems," *Sustain.*, vol. 13, no. 16, 2021, doi: 10.3390/su13169459.
- [27] M. Ali, H. Kotb, K. M. Aboras, and N. H. Abbacy, "Design of cascaded pi-fractional order PID controller for improving the frequency response of the hybrid microgrid system using gorilla troops optimizer," *IEEE Access*, vol. 9, pp. 150715–150732, 2021, doi: 10.1109/ACCESS.2021.3125317.
- [28] M. A. El-Dabah, M. H. Hassan, S. Kamel, and H. M. Zawbaa, "Robust Parameters Tuning of Different Power System Stabilizers Using a Quantum Artificial Gorilla Troops Optimizer," *IEEE Access*, vol. 10, no. June, pp. 82560–82579, 2022, doi: 10.1109/ACCESS.2022.3195892.
- [29] S. Falahati, S. A. Taher, and M. Shahidehpour, "Grid secondary frequency control by optimized fuzzy control of electric vehicles," *IEEE Trans. Smart Grid*, vol. 9, no. 6, pp. 5613–5621, 2018, doi: 10.1109/TSG.2017.2692265.
- [30] M. U. Jan, A. Xin, H. U. Rehman, M. A. Abdelbaky, S. Iqbal, and M. Aurangzeb, "Frequency Regulation of an Isolated Microgrid with Electric Vehicles and Energy

- Storage System Integration Using Adaptive and Model Predictive Controllers,” *IEEE Access*, vol. 9, no. January, pp. 14958–14970, 2021, doi: 10.1109/ACCESS.2021.3052797.
- [31] A. Safari, F. Babaei, and M. Farrokhifar, “A load frequency control using a PSO-based ANN for micro-grids in the presence of electric vehicles,” *Int. J. Ambient Energy*, vol. 42, no. 6, pp. 688–700, 2021, doi: 10.1080/01430750.2018.1563811.
- [32] A. Latif, S. M. S. Hussain, D. C. Das, and T. S. Ustun, “Design and implementation of maiden dual-level controller for ameliorating frequency control in a hybrid microgrid,” *Energies*, vol. 14, no. 9, 2021, doi: 10.3390/en14092418.
- [33] J. M. R. Chintu and R. K. Sahu, *Design and Implementation of ADE Based Cascade PD-PI Controller for AGC of Multi-area Power System*. Springer International Publishing, 2020. Do: 10.1007/978-3-030-30271-9_5.
- [34] D. E. Olivares *et al.*, “Trends in microgrid control,” *IEEE Trans. Smart Grid*, vol. 5, no. 4, pp. 1905–1919, 2014, doi: 10.1109/TSG.2013.2295514.
- [35] G. I. Said and A. E. Hassanien, *Optimizer and Its Application for Fundus*, vol. 2, no. Cic. Springer International Publishing, 2022. Do: 10.1007/978-3-030-89701-7.
- [36] E. M. Ahmed, A. Elmelegi, A. Shawky, M. Aly, W. Alhosaini, and E. A. Mohamed, “Frequency Regulation of Electric Vehicle-Penetrated Power System Using MPA-Tuned New Combined Fractional Order Controllers,” *IEEE Access*, vol. 9, pp. 107548–107565, 2021, doi: 10.1109/ACCESS.2021.3100800.
- [37] I. Şerban and C. Marinescu, “Aggregate load-frequency control of a wind-hydro autonomous microgrid,” *Renew. Energy*, vol. 36, no. 12, pp. 3345–3354, 2011, doi: 10.1016/j. Rene ne. 2011. 05. 012.
- [38] R. K. Khadanga, A. Kumar, and S. Panda, “A novel sine augmented scaled sine cosine algorithm for frequency control issues of a hybrid distributed two-area power system,” *Neural Comput. Appl.*, vol. 0123456789, 2021, doi: 10.1007/s00521-021-05923-w.
- [39] G. I. Said and A. E. Hassanien, “A Novel Chaotic Artificial Gorilla Troops Optimizer and Its Application for Fundus Images Segmentation BT - Proceedings of the International Conference on Advanced Intelligent Systems and Informatics 2021,” 2022, pp. 318–329.